

A New Enantiornithine from the Yixian Formation with the First Recognized Avian Enamel Specialization

Author(s): Jingmai K. O'Connor , Yuguang Zhang , Luis M. Chiappe , Qingjin Meng , Li Quanguo , and Liu Di

Source: Journal of Vertebrate Paleontology, 33(1):1-12. 2013.

Published By: The Society of Vertebrate Paleontology

URL: <http://www.bioone.org/doi/full/10.1080/039.033.0120>

BioOne (www.bioone.org) is a nonprofit, online aggregation of core research in the biological, ecological, and environmental sciences. BioOne provides a sustainable online platform for over 170 journals and books published by nonprofit societies, associations, museums, institutions, and presses.

Your use of this PDF, the BioOne Web site, and all posted and associated content indicates your acceptance of BioOne's Terms of Use, available at www.bioone.org/page/terms_of_use.

Usage of BioOne content is strictly limited to personal, educational, and non-commercial use. Commercial inquiries or rights and permissions requests should be directed to the individual publisher as copyright holder.

A NEW ENANTIORNITHINE FROM THE YIXIAN FORMATION WITH THE FIRST RECOGNIZED AVIAN ENAMEL SPECIALIZATION

JINGMAI K. O'CONNOR,^{*,1,2} YUGUANG ZHANG,³ LUIS M. CHIAPPE,¹ QINGJIN MENG,³ LI QUANGUO,³ and LIU DI³

¹Dinosaur Institute, Natural History Museum of Los Angeles County, 900 Exposition Boulevard, Los Angeles, CA 90007, U.S.A.;

²Key Laboratory of Evolutionary Systematics of Vertebrates, Institute of Vertebrate Paleontology and Paleoanthropology, 142 Xizhimenwai Dajie, Beijing, China 100044, jingmai.oconnor@gmail.com;

³Beijing Museum of Natural History, 126 Tianqiao South Street, Beijing, China 100050

ABSTRACT—We report on a new enantiornithine bird, *Sulcavis geeorum*, gen. et sp. nov., from the Jehol Group of north-eastern China. The fossil preserves robust teeth with longitudinal grooves radiating from the occlusal tip preserved in the enamel on the lingual surface. This is the first known occurrence of specialized tooth enamel within Aves. Compared with other Mesozoic groups, stomach contents are hardly ever preserved within enantiornithine specimens; therefore, this new tooth morphology reveals new evidence regarding the diversity of trophic niches occupied by the clade.

SUPPLEMENTAL DATA—Supplemental materials are available for this article for free at www.tandfonline.com/UJVP

INTRODUCTION

New species of fossil bird are being uncovered from the Jehol Group in northeastern China at an unprecedented rate and the recognized range of morphological variation among Early Cretaceous birds continues to grow. During the last two decades, over 40 avian species have been named (Zhou and Zhang, 2006a). More than half of these species are referable to Enantiornithes, the most speciose Cretaceous clade of birds and the sister taxon to Ornithuromorpha, the lineage that includes modern birds. The Jehol Group is also important because specimens from these deposits preserve more than osteological morphology, and reveal aspects of the biology of these extinct birds, such as plumage, diet, ecology, life history, and development (Zhang and Zhou, 2000; Hou et al., 2004; Zhou and Zhang, 2004; Chiappe et al., 2008; O'Connor et al., 2009).

Approximately half of all enantiornithines are known from the Jehol Group, and nearly every species is represented by a partial to nearly complete articulated skeleton, often preserving integument (Zhou and Zhang, 2006a; Chiappe, 2007). Unfortunately, not one published specimen preserves direct evidence of trophic habit such as stomach contents, although numerous ornithuromorph specimens preserve ingested remains and other indicators of diet, with geo-gastroliths being particularly common (Zhou et al., 2004; Zhou and Zhang, 2006b). The only two enantiornithine specimens that preserve such evidence are from outside China: the holotype of *Eoalulavis hoyasi* Sanz, Chiappe, Pérez-Moreno, Buscalioni, Moratalla, Ortega, and Poyato-Ariza, 1996, preserves the exoskeletal remains of crustaceans in the thoracic cavity, interpreted as stomach contents, suggesting an aquatic feeding habitat (Sanz et al., 1996); the holotype of *Enantiophoenix electrophyla* Cau and Arduini, 2008, preserves small inclusions of amber associated with the skeleton, which have been interpreted as ingested items and indicative of a diet that included sap (Dalla Vecchia and Chiappe, 2002).

To date, the only way to infer the trophic habit of enantiornithines from the Jehol Group is through their cranial or den-

tal morphology. Enantiornithines exhibit a wide range of cranial morphologies (O'Connor and Chiappe, 2011) and the long rostrum of some of these taxa has been used to infer specific trophic specializations (Zhang et al., 2000; Hou et al., 2004; Morschhauser et al., 2009; O'Connor et al., 2009). A diversity of dental shapes, sizes, and patterns are also apparent in the Jehol enantiornithines (O'Connor and Chiappe, 2011). However, although the teeth range in overall morphology, caudal curvature, lateral compression, and size, no previous specimens have preserved ridges, striations, denticles, or any other form of dental ornamentation. Likewise, no Jehol enantiornithine preserves edentulous jaws, although this is present in a diversity of basal ornithuromorphs (e.g., *Archaeorhynchus spathula* Zhou and Zhang, 2006b, *Hongshanornis longicresta* Zhou and Zhang, 2005), the confuciusornithiforms (Chiappe et al., 1999), and *Zhongjianornis zhengi* Zhou, Zhang, and Li, 2010 (Zhou and Zhang, 2005; Zhou and Zhang, 2006b; Zhou et al., 2010), all from the Jehol Group.

In this paper, we describe the morphology of a new enantiornithine specimen (BMNH Ph-000805) from the Jehol Group, which presents a unique dental specialization—one that is suggestive of a durophagous diet. BMNH Ph-000805 appears to be closely related to the recently described *Shenqiornis mengi* Wang, O'Connor, Zhao, Chiappe, Gao, and Cheng, 2010, with which it shares aspects of the dental morphology, and the two taxa are included in a phylogenetic analysis to explore this potential relationship. The new specimen, although more fragmentary than the holotype of *Shenqiornis mengi*, also reveals distinct morphologies in the skull and postcranial skeleton that suggest that it represents a new taxon.

Institutional Abbreviations—**BMNH**, Beijing Museum of Natural History, Beijing, China; **LACM**, Natural History Museum of Los Angeles County, Los Angeles, U.S.A.

SYSTEMATIC PALEONTOLOGY

AVES Linnaeus, 1758

PYGOSTYLIA Chiappe, 2002

*Corresponding author.

ORNITHOTHORACES Chiappe, 1995

ENANTIORNITHES Walker, 1981

SULCAVIS GEEORUM, gen. et sp. nov.

(Figs. 1, 2)

Holotype—BMNH Ph-000805, a slab containing a nearly complete adult or subadult individual, generally preserved in ventral

view, with poorly preserved feathers around the skull and shoulders (Figs. 1, 2). An epoxy resin cast of the holotype is deposited in the collection of the Natural History Museum of Los Angeles County under the number LACM 7868 /155179.

Etymology—*Sulcavis*, Latin 'sulcus' meaning groove, and 'avis' meaning bird, refers to the grooves on the teeth that make



FIGURE 1. Photograph of the holotype of *Sulcavis geeorum*, gen. et sp. nov., BMNH Ph-000805.

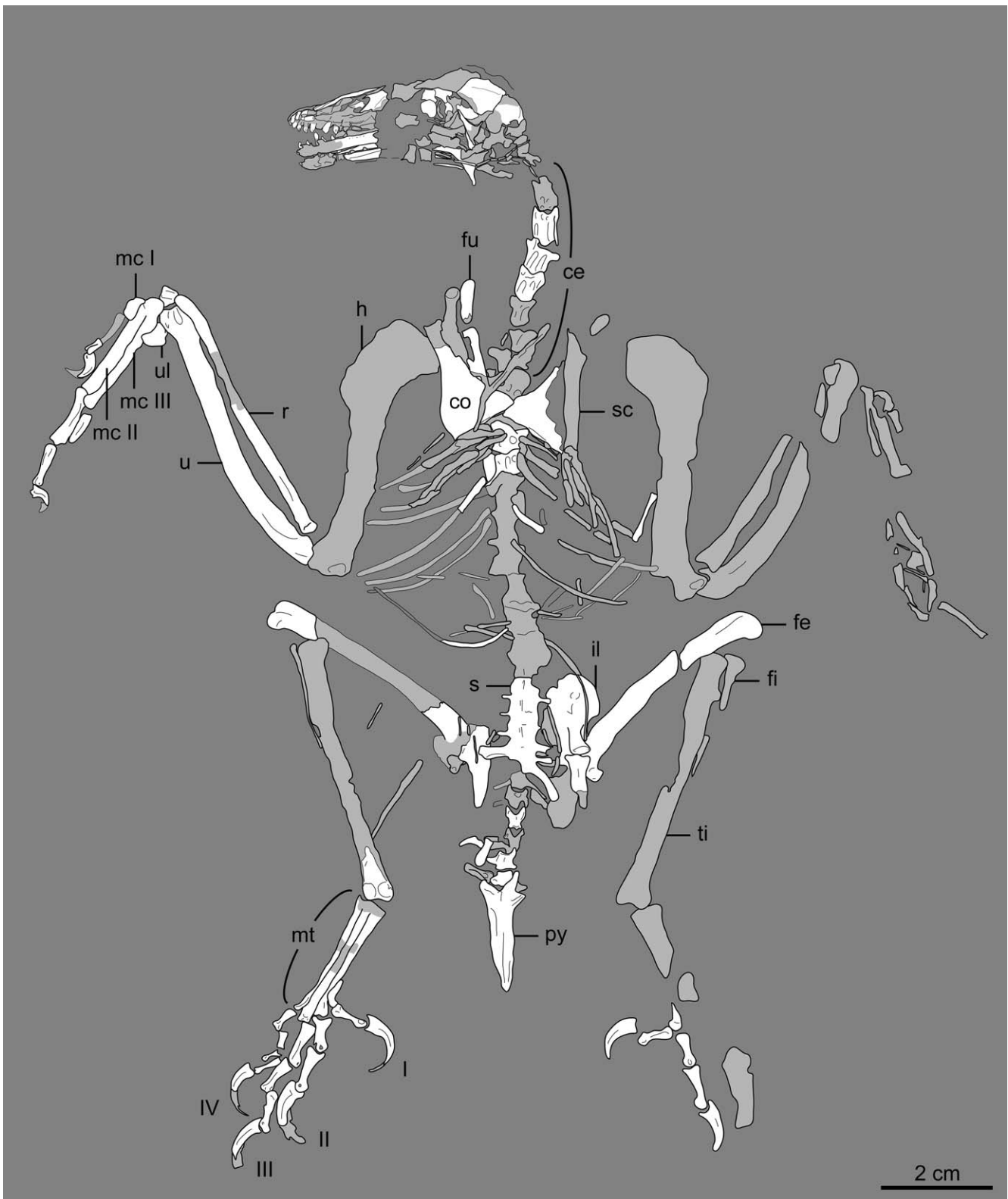


FIGURE 2. Camera lucida drawing of the holotype of *Sulcavis georum*, gen. et sp. nov., BMNH Ph-000805. Light gray indicates areas of poor preservation; dark gray indicates matrix. **Abbreviations:** *ce*, cervical vertebrae; *co*, coracoid; *fe*, femur; *fi*, fibula; *fu*, furcula; *h*, humerus; *il*, ilium; *mc*, metacarpal; *mc I*, alular digit; *mc II*, major digit; *mc III*, minor digit; *mt*, metatarsals; *py*, pygostyle; *r*, radius; *s*, synsacrum; *sc*, scapula; *ti*, tibiotarsus; *u*, ulna; *ul*, ulnare.

TABLE 1. Comparison of select measurements (in mm) of BMNH Ph000805 and DNHM D2950/1.

Element	BMNH Ph000805	DNHM D2950/1
Synsacrum	19.3	23.4
Pygostyle	19.6	—
Coracoid, length, left	24.8	26.2
Coracoid, width, right	12.1	(9.9)
Scapula, right	34.9	39.3
Furcula	27.5	28.9
Length, right ramus	19.5	18.7
Length, hypocleidium	8.3	8*
Interclavicular angle	60°	45°*
Humerus, right	46.5	46.6
Ulna, right	51.1	46.8
Ulnar shaft width	4.7	4.1
Radius, right	47.7	45.8
Radial shaft width	2.6	2.2
Ilium, left	26.5	27*
Femur, left	41.3	38.8*
Tibiotarsus, right	47.3	(33)
Fibula, right	18.9	—
Tarsometatarsus, right	24.85	25
Metatarsal I	5	7
Metatarsal II	21.6	22.4*
Metatarsal III	24.3	25
Metatarsal IV	22.6	22.8
Intermembral index (humerus + ulna)/(femur + tibiotarsus)	1.1	—

Measurements from DNHM D2950/1 are compiled from both slabs based on best preservation. Parentheses denote incomplete bones; an asterisk indicates estimated measurements.

the new taxon unique. The species name, *georum*, is in honor of the Gee family of La Cañada, U.S.A., for their generous contributions in support of Mesozoic bird research.

Locality and Horizon—Near Lamadong Village, Jianchang County, Huludao City, Liaoning Province, China. Yixian Formation, Early Cretaceous.

Diagnosis—A medium-sized enantiornithine (Table 1) with the unique combination of the following morphologies: robust teeth with caudally recurved apices, ‘D’-shaped cross-section with flat lingual margin, and lingual face with longitudinal grooves radiating from the occlusal tip (autapomorphy); broad nasal with short, tapered, rostrally directed maxillary process; caudal-most transverse processes of synsacrum extending far beyond the caudal articular surface of their respective centra; scapula with long and delicate acromion process; convex lateral margin of the coracoid; medial angle of coracoid expanded; ‘Y’-shaped furcula with blunt omal apices; alular claw larger than that of the major digit; pedal digit II hypertrophied; deep pits for the collateral ligament and lateral ridges present on pedal claws.

DESCRIPTION

Anatomical nomenclature primarily follows Baumel and Witmer (1993); English translations are used for skeletal terms, whereas Latin is retained for muscles.

Skull

The skull is preserved in left lateral view (Fig. 3). Some portions of the lateral surface are not preserved so that certain skull elements are visible in medial view. The caudal half of the skull is poorly preserved, and a large crack cuts dorsoventrally through the skull.

The premaxillae are poorly preserved. The degree of rostral fusion is uncertain; however, we interpret the nasal (frontal) processes as unfused to one another. This is based on the interpreta-

tion of the only well-preserved nasal process as that of the right side, which bears a natural medial edge for the contact with its left counterpart. This interpretation is also supported by the presence of a bone fragment, presumably belonging to the left nasal process of the premaxilla, which is displaced ventrally from the center of the medial surface of the right nasal process. The nasal processes of the premaxillae did not contact the frontals as they do in modern birds. The roots of three teeth are preserved in lateral view in the left premaxilla; an additional caudal-most tooth is inferred to have been present based on what is interpreted as the abraded medial surface of an empty alveolus just ventral to the split between the nasal and maxillary processes of the premaxilla. The teeth of the right upper jaw are exposed in medial view, revealing their flat lingual surfaces (Fig. 3A). The rostral-most four teeth are interpreted as premaxillary, although the location of the premaxilla-maxilla contact is not clearly preserved. Nonetheless, the preserved morphology of the premaxilla and the placement of the rostral-most teeth indicate that this bone was rostrally restricted, forming at most one-quarter of the rostral margin.

The right nasal is exposed in dorsal view. It is a broad bone, suggesting a wide rostrum, with a long internasal edge, indicating an extensive contact with its left counterpart. The premaxillary process of this bone tapers rostrally, although its rostral end is covered. The nasal reaches its maximal width at the level of the maxillary process, which is short and sharply tapered rostrally. The morphology of the nasal indicates that this bone formed the rounded caudal margin of the external nares.

Both maxillae are preserved; the left is poorly preserved and apparently in lateral view, whereas the right is visible in medial and slightly ventral view. The right maxilla is preserved in articulation with the right premaxilla. The maxilla forms most of the ventral margin of the rostrum. It is difficult to count the total number of teeth carried by the maxilla because the precise contact with the premaxilla is unclear and there are some disarticulated teeth. Anywhere from four to six maxillary teeth are estimated to be present. The teeth are exposed in both lingual and labial views, and have flat lingual surfaces and strongly convex labial surfaces. The labial surfaces are also fairly smooth, whereas the lingual surfaces bear distinct narrow longitudinal grooves that radiate from the apex, and extend throughout the length of the tooth crown; these grooves are particularly evident in the premaxillary teeth. Grooves have not been reported in the enamel of any other Mesozoic bird. Neither the rostral nor caudal articulations of the maxilla can be discerned (the former due to overlap with other elements and the latter to due to lack of preservation).

The orbital region of the skull is poorly preserved (Fig. 3B). A few elements preserved in the orbital fenestra are interpreted as scleral ossicles. No apparent lacrimal is preserved. A large triangular bone in the crushed caudal margin of the orbit is interpreted as the displaced left postorbital. A similar bone is preserved in the holotype of *Shenqiornis mengi* (see O’Connor and Chiappe, 2011). The frontal process of this bone is longer than the parietal process; together they define the concave margin of the supratemporal fossa. The jugal process of the postorbital is extensive. The ventrorostral portion of this process abuts with what appears to be a different bone (as opposed to a portion of the same postorbital), here interpreted as the postorbital process of the jugal—the jugal bar is not preserved. The large size and morphology of the postorbital suggests that the infratemporal fenestra was nearly fully enclosed—presumably fully enclosed if the interpretation of the postorbital process of the jugal is correct. The fact that the longest process of the triradiate postorbital of *Sulcavis* appears to be the frontal process complicates the interpretation of the seemingly disarticulated postorbital of *Shenqiornis* (O’Connor and Chiappe, 2011), and future specimens may be required to clarify the orientation of this bone in the latter taxon.

The frontal is very poorly preserved and, from its size, potentially incomplete; the caudal half of the frontal may be covered

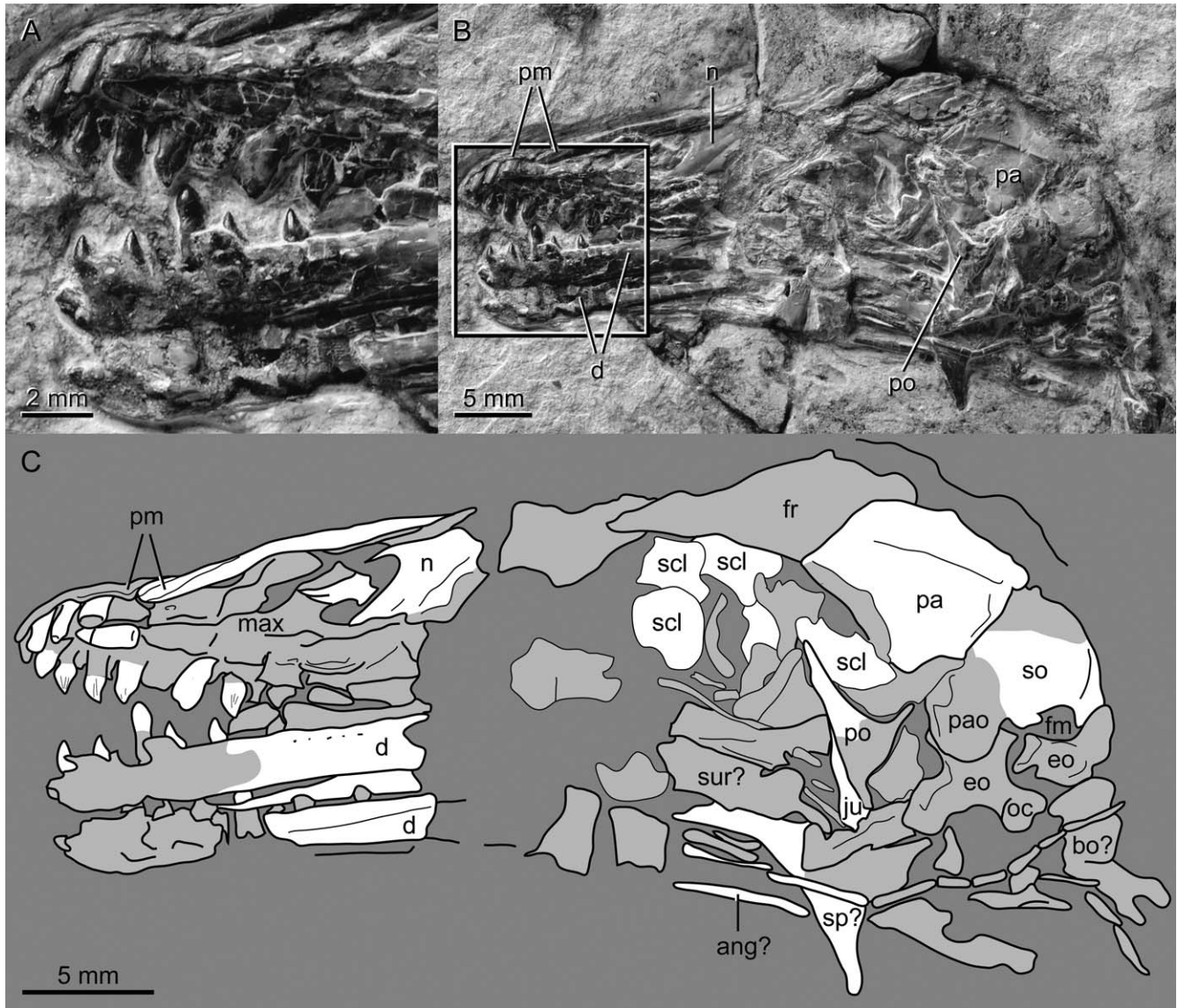


FIGURE 3. Detail of skull of BMNH Ph-000805. **A**, proximal half of rostrum; **B**, entire skull, right lateral view; **C**, interpretative drawing. Light gray indicates areas of poor preservation; dark gray indicates matrix. **Abbreviations:** **ang?**, angular?; **bo?**, basioccipital; **d**, dentary; **eo**, exoccipital; **fr**, frontal; **fm**, foramen magnum; **ju**, postorbital process of the jugal; **max**, maxilla; **n**, nasal; **oc**, occipital condyle; **pa**, parietal; **pao**, paraoccipital process; **pm**, premaxilla; **po**, postorbital; **scl**, scleral ossicle; **so**, supraoccipital; **sp?**, splenial; **sur?**, surangular. (Color figure available online.)

by the parietal due to displacement of the occipital region. The parietal is comparatively well preserved—it is large and quadrangular, more than twice the size of the supraoccipital with which it articulates. A ridge intersects this bone; whether this is the sagittal nuchal crest or results from an underlying bone cannot be determined. Interpretations of the caudal portion of the skull are complicated by poor preservation and partial disarticulation (Fig. 3). The supraoccipitals are preserved, fused into a single element in caudal view, with a sagittally located cerebral prominence that reaches the foramen magnum. The right exoccipital is disarticulated, obscuring the size and shape of the foramen magnum. The left exoccipital is in caudolateral view in articulation with the ventrolaterally tapering paraoccipital process of the supraoccipital. Only the right exoccipital contribution of the occipital condyle is preserved; although incomplete, the occipital condyle appears proportionately large relative to the foramen

magnum, as in other enantiornithines (e.g., *Shenqiornis*, *Vescornis*) (O'Connor and Chiappe, 2011). A poorly preserved bone ventral to the right exoccipital may be part of the basioccipitals.

The two dentaries are not fused rostrally and no predentary bone is preserved, morphologies consistent with other enantiornithines. The left dentary is preserved in lateral view, whereas the right is preserved in medial view (Fig. 3B). Seven teeth are preserved in the left dentary. A row of small foramina marks the lateral margin of the dentary, just ventral to the dentigerous margin. The right dentary preserves at least 7 teeth but we estimate that 9 or 10 may have been present in total. Meckel's groove is visible on the right dentary, restricted to the caudal half of the bone and tapering rostrally. The caudal half of both dentaries is not preserved, and interpretation of the fragmentary postdentary bones is equivocal. Several long, thin bones may represent the angular or portions of the hyoid bones—one of

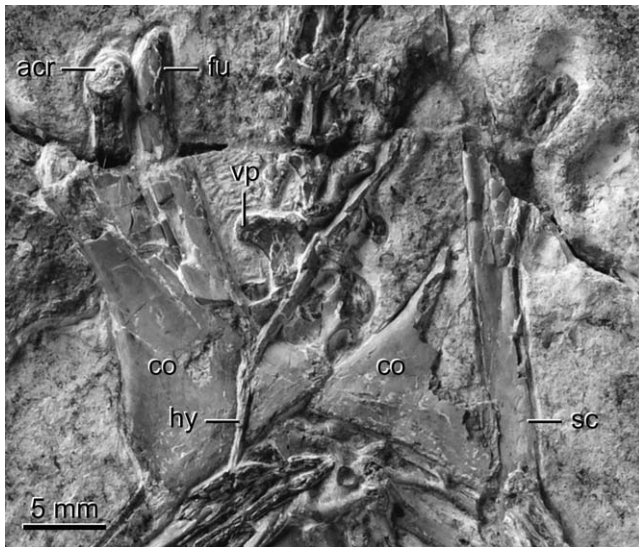


FIGURE 4. Detail photograph of the pectoral girdle of BMNH Ph-000805. **Abbreviations:** *acr*, acromion process; *co*, coracoid; *fu*, furcula; *hy*, hypocleidium; *sc*, scapula; *vp*, ventral process. Other abbreviations, see Figure 3. (Color figure available online.)

these bones is clearly preserved beneath the occipital condyle. A triangular bone may be a caudally displaced splenial.

Axial Skeleton

Six articulated cervical vertebrae are clearly preserved in ventral view (Fig. 1); the proximal-most cervical vertebrae (the atlas, axis, and possibly one additional cervical) cannot be differentiated, and thus the total number of cervicals is estimated to be eight to nine. The preserved cervicals have in situ and presumably fused (fully articulated, no sutures but preservation not clear enough to determine unequivocally) costal processes that are nearly as long as the centrum—these processes are unfused in the last two vertebrae. Small carotid processes are located medial to the proximal ends of the costal processes. Given the complete articulation of the series, we cannot determine if the vertebrae were truly heterocoelic. The cervical centra are keeled ventrally, flanked by ventral longitudinal recesses, although the height of this keel cannot be determined in most vertebrae. In the last preserved cervical (exposed in lateral view), the ventral process projects rostrally, extending slightly beyond the ventral edge of the cranial articular surface, and tapers caudally (Fig. 4). This last cervical clearly marks the cervicothoracic transition.

Caudal to the last cervical vertebrae, five poorly exposed articulated thoracic vertebrae are visible, the first in left lateral view and the last in ventral view. The penultimate of these vertebrae exhibits a broad excavation on the side of the centrum and the last two exhibit centrally located parapophyses, as seen in other enantiornithines (Chiappe and Walker, 2002). The rest of the series is very poorly preserved in articulation with the synsacrum.

The synsacrum comprises seven or eight vertebrae (Fig. 5). The transverse processes are short and delicate along the proximal half of the synsacrum, and larger and more robust on the distal half. All but the last transverse processes are directed perpendicular to the sacral axis and would have braced the pelvic girdle. The last two transverse processes are very long, extending far beyond the caudal articular surface of the synsacrum, and are strongly deflected caudally.

At least five free caudal vertebrae are preserved in ventral view (Fig. 5). The prezygapophyses are more elongate than the postzy-

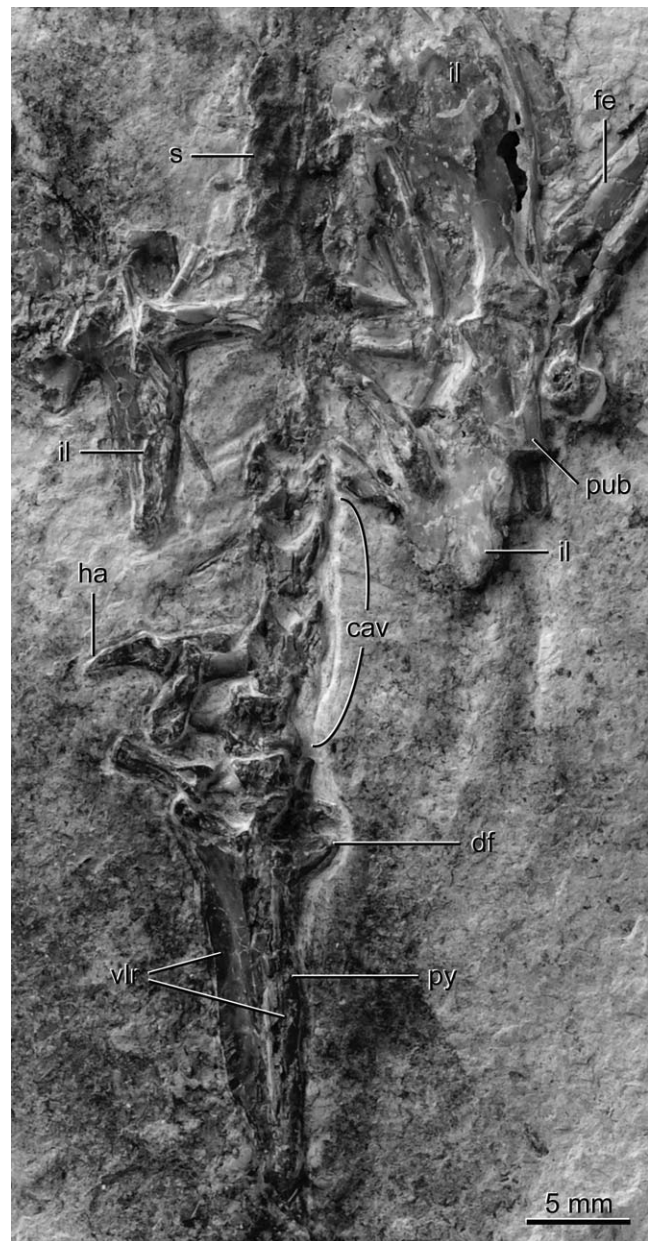


FIGURE 5. Detail photograph of the pelvic girdle of BMNH Ph-000805. **Abbreviations:** *cav*, caudal vertebrae; *df*, dorsal fork; *fe*, femur; *ha*, hemal arch; *il*, ilium; *pub*, pubis; *py*, pygostyle; *s*, synsacrum; *vlr*, ventrolateral process. Other abbreviations, see Figure 3. (Color figure available online.)

gapophyses. The last two caudals bear short, laterally directed transverse processes; those of the proximal vertebrae are not preserved. Several isolated elements preserved beside the caudal series are interpreted as hemal arches; they are somewhat longer than the adjacent centra and distally are bluntly tapered.

The pygostyle is triangular in shape, preserved in ventral view (Fig. 5). The morphology of the pygostyle is similar to that of other enantiornithines. Proximally, it possesses a pair of dorsal processes, and the lateral edges bear lateroventrally directed processes. The right lateroventral process is abraded off. As in most other enantiornithines, the pygostyle is constricted along its distal fifth; however, this constriction is more distally located and not as abrupt as in *Rapaxavis pani* Morschhauser, Varricchio, Gao,

Liu, Wang, Cheng, and Meng, 2009, and other enantiornithines (O'Connor et al., 2011b).

Thoracic Girdle

The coracoids are preserved in ventral view, precluding observation of the dorsal surface (Fig. 4). However, a deep fossa like that of *Enantiornis leali* Walker, 1981, was most likely absent (Chiappe and Walker, 2002). The coracoids are distally broad and very wide, expanding rapidly from the rod-like neck, which forms the proximal one-third of the bone. They apparently lack a procoracoid process, and the presence of a supra-coracoidal nerve foramen and/or medial groove cannot be determined. The lateral margins of the coracoids are strongly convex over the distal third of the bone, consistent with most enantiornithines, and most strongly resembling the coracoids of *Eoalulavis hoyasi*. The coracoids are preserved with their medial angles overlapping—however, the right coracoid is slightly displaced medially and we interpret that the coracoids would not have overlapped in life. The distal fifth of the medial margin is slightly convex, contributing to the expanded sternal margin. The sternal margin is straight to slightly concave and a lateral process is absent.

The coracoids are overlain by the furcula, which is 'Y'-shaped with an elongate hypocleidium at least half the length of the furcular rami (Fig. 4). Although the furcula is exposed in ventral view, breakage reveals that it was excavated dorsolaterally, as in other enantiornithines (Chiappe and Calvo, 1994; Martin, 1995; Chiappe and Walker, 2002). The omal tips are blunt and curved slightly medially.

The scapulae are largely covered by other elements; however, the elongate acromion of the right scapula is exposed; the process is long and delicate, as in *Eoalulavis hoyasi*, and the proximal end of the acromion is expanded into a rounded surface that may have articulated with the furcula (Fig. 4) (Sanz et al., 1996). A scapular costal groove, reported for other enantiornithines (Chiappe and Walker, 2002), is absent.

No direct information regarding the morphology of the sternum is preserved (Fig. 1). A few fragments preserved distal to the coracoids may represent the rostral margin of the sternum, or alternatively they may be poorly preserved thoracic ribs. However, the preserved position of the coracoids suggests that the rostral margin of the sternum would have defined an approximately 100° angle with the apex at midpoint, similar to *Rapaxavis pani*, as opposed to having a rounded margin as in some other enantiornithines (e.g., *Longipteryx chaoyangensis* Zhang, Zhou, Hou, and Gu, 2000) (O'Connor et al., 2011b). Gastralia are preserved, some of them overlapping the pelvic girdle.

Thoracic Limb

The left wing is poorly preserved and all morphological information comes from the right wing (Fig. 6). The proximal margin of the humerus, exposed cranially, is typically enantiornithine—it is centrally concave, with raised ventral and dorsal ends. The proximoventral margin of the humerus projects strongly ventrally, as noted for *Zhongjianornis yangi* (Zhou et al., 2010; O'Connor et al., 2011a) and the basal ornithuromorph *Schizooura lii* Zhou, Zhou, and O'Connor, 2012. The deltopectoral crest is more than one-third the length of the humerus, nearly the same width as the shaft, ending abruptly. The ulna is longer than the humerus and bowed proximally; the radius is straight.

The ulnare is triangular, with only a shallow incisure. The radiale is quadrangular and the exposed surface bears a median groove. The alular metacarpal was clearly unfused to the other elements of the metacarpus (Fig. 6). The semilunate carpal and major and minor metacarpals also appear to be unfused to each other, although the preservation makes such interpretation

equivocal. The alular metacarpal is rectangular, although in profile the cranial margin is slightly convex in its middle portion, possibly representing an incipient extensor process. The proximal phalanx of this digit appears to be slightly bowed craniocaudally; the second phalanx is a large claw with a recurved horny sheath. The alular digit has equal distal extent with the major metacarpal. The proximal margin of the major metacarpal is located proximal to that of the minor metacarpal; however, this region of the carpometacarpus is poorly preserved. The minor metacarpal extends distally farther than the major metacarpal, as in all other enantiornithines (Martin, 1995; Chiappe and Walker, 2002). The minor metacarpal is less than half the width of the major metacarpal, and the two are not separated by an intermetacarpal space, although this may be a taphonomic artifact. The major digit is composed of three phalanges, which decrease in length distally (Fig. 6). The first phalanx of the major digit is cranially expanded along its length, forming a blunt longitudinal ridge comparable to the cranial phalangeal ball (pila cranialis phalangeis) that reinforces the digit in living birds (Baumel and Witmer, 1993). The caudal margin of the first phalanx constricts just proximal to its distal articulation; the distoventral margin of the constriction forms a small tubercle. The claw is smaller than that of the alular digit, but also strongly recurved, with the horny sheath preserved. A single phalanx is preserved for the minor digit. It is half the length of the proximal phalanx of the major digit, with a straight cranial margin and a slightly concave caudal margin. The distal end of this phalanx is blunt.

Pelvic Girdle

The ilia and synsacrum are unfused, and the pelvic elements appear unfused at the level of the acetabulum (Fig. 5). What is preserved of the pelvic girdle remains in nearly complete articulation. The left ilium is completely preserved, whereas only the postacetabular wing is preserved on the right. The proximal margin of the preacetabular wing is rounded in ventral view; in lateral view, the postacetabular wing is triangular, distally tapering bluntly. The proximal portion of the left pubis is preserved, unfused to but in articulation with the ilium; no pectineal process is present. The pubic shaft is proximally robust but it narrows distally. A piece of the left ischium is preserved but reveals no anatomical information.

Pelvic Limb

The femora are preserved in near articulation with the pelvis (Fig. 5). They are straight and rather slender. The tibiotarsi are only 10% longer than the femora. The left is poorly preserved, yielding no information; the right is preserved in cranial view (Fig. 7). The proximal cranial surface is abraded and no cnemial crests are preserved; the short fibular crest extends less than one-third the length of the tibiotarsus. Distally, the condyles are subequal in size, bulbous, and separated by a narrow incisure. A tall triangular ascending process is visible on the cranial surface proximal to the condyles, indicating that fusion of the tibia with the proximal tarsals was not complete in this specimen at the time of death. As preserved, the fibula is approximately half the length of the tibiotarsus.

The proximal ends of metatarsals II–IV are fused to the distal tarsals; the shafts of these metatarsals appear unfused along their entire length (Fig. 7). A very slight intercotylar eminence is present; the lateral margin of the proximal articular surface of the tarsometatarsus (lateral cotyla) projects proximally to the same level as the intercotylar eminence (and more strongly than the medial margin). No tubercle for the m. tibialis cranialis is preserved on the cranial surface of metatarsals II or III; damage to the cranial surface of portions of metatarsal II and III suggests that if a tubercle was present, it was fairly distally located, as in *Yungavolucris brevipedalis* Chiappe, 1993. Proximally, the

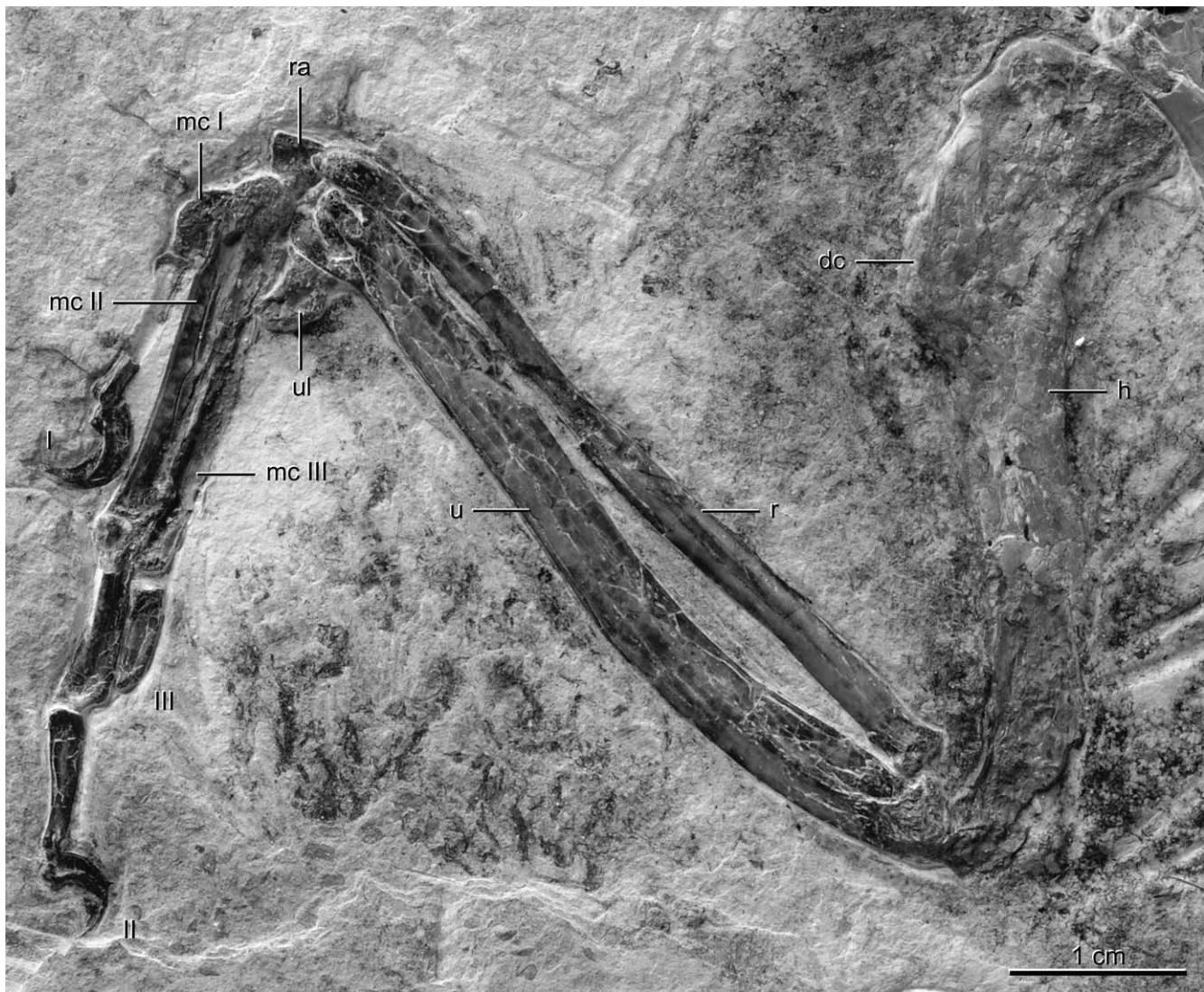


FIGURE 6. Detail photograph of the right wing of BMNH Ph-000805. **Abbreviations:** **dc**, deltopectoral crest; **h**, humerus; **mc I**, alular digit; **mc II**, major digit; **mc III**, minor digit; **r**, radius; **ra**, radiale; **u**, ulna; **ul**, ulnare. Other abbreviations, see Figure 3. (Color figure available online.)

cranial surface of metatarsal III is strongly convex, as in avisaurid enantiornithines (Chiappe, 1992), and all three metatarsals are in the same plane. Metatarsal III extends the farthest distally, followed by IV and then II. The trochlea of metatarsal II is slightly wider than that of metatarsal III, as in many enantiornithines (Chiappe, 1993; Chiappe and Walker, 2002); the trochlea is poorly differentiated into two condyles and the distal margin is slightly angled proximomedially-distolaterally. The trochlea of metatarsal III forms well-developed trochlear condyles in which the lateral condyle projects distal to the medial condyle. A well-developed cranial trochlear depression (*depressio trochlea cranialis*) is present. The trochlea of metatarsal IV is non-inglymously, reduced to a single condyle that is mediolaterally compressed, with a concave lateral surface. Just proximal to the condyle, the craniomedial surface has a slight projection that extends slightly onto the cranial surface of the metatarsal III and may have demarcated a distal vascular foramen as in *Soroavisaurus australis* Chiappe, 1993.

Metatarsal I clearly articulates with the medial surface of metatarsal II. Metatarsal I is 'P'-shaped; unfortunately, the dis-

tal articular surface for the digit I is covered and the relationships between the planes of articulation cannot be determined. All the phalanges bear deep flexor pits. The proximal phalanx of digit I is approximately the same length as that of digit II but half the width. The unguis phalanx of the first digit is subequal in size to that of the third digit. Digit II is more robust than the other digits. The first phalanx is short and fat, the proximal articular surface expanded; the intermediate phalanx is 50% longer, although not as wide as the proximal phalanx. The unguis is the largest in the foot. The proximal phalanx of the third digit is subequal in length to the intermediate phalanx of digit II, but more slender. The following two phalanges are shorter and subequal. All the phalanges of the fourth digit are short; the proximal and penultimate phalanges are subequal in length, whereas the two intermediate phalanges are shorter and more delicate. The unguis phalanx of digit IV is the smallest in the foot. All the unguis are large and recurved, compared with those of sympatric ornithuromorphs, and bear lateral ridges, as in some other enantiornithines (i.e., *Rapaxavis pani* and *Shanweinia cooperorum* O'Connor, Wang, Chiappe, Gao, Meng, Cheng, and Liu, 2009) (O'Connor et al., 2009,

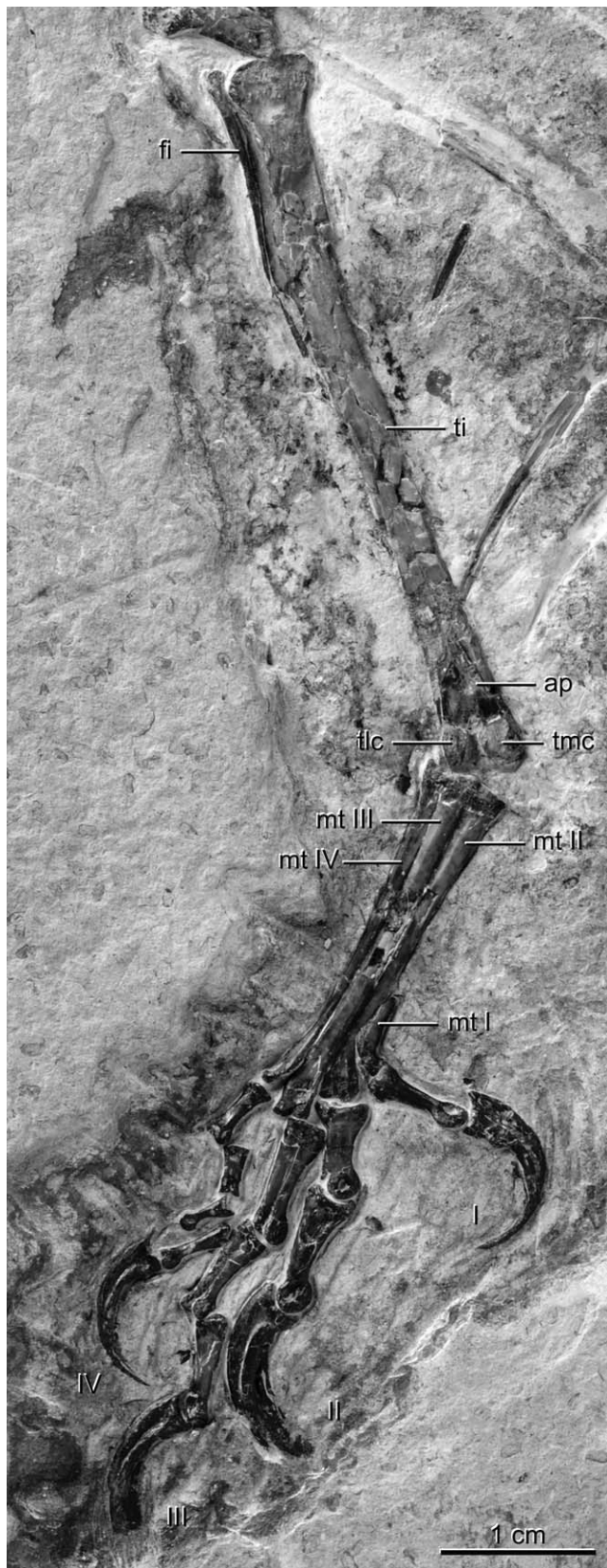


FIGURE 7. Detail photograph of the right foot of BMNH Ph-000805. **Abbreviations:** ap, ascending process of the astragalus; fi, fibula; mt, metatarsals; ti, tibia; tlc, lateral condyle of the tibiotarsus; tmc, medial condyle. Other abbreviations, see Figure 3. (Color figure available online.)

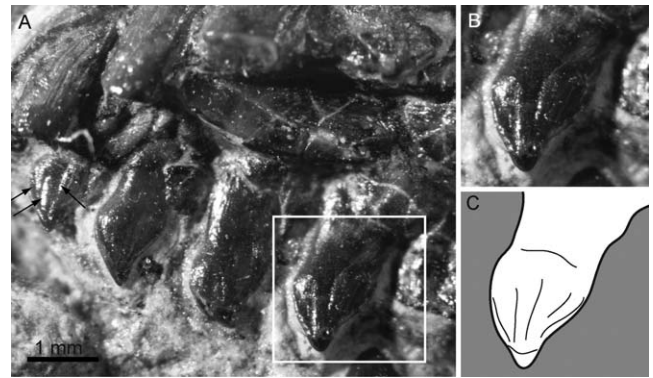


FIGURE 8. Details of the right premaxillary-maxillary teeth of BMNH Ph-000805 in lingual view. **A**, photograph of the dentition at the right premaxilla-maxilla contact, in lingual view box indicates area expanded in **B**; **B**, close up of maxillary tooth; **C**, interpretative drawing of maxillary tooth. Arrows indicate the longitudinal grooves. (Color figure available online.)

2011b). Large strongly recurved horny sheaths are preserved with the unguals.

DISCUSSION

Phylogenetic Hypothesis

BMNH Ph-000805 is considered to be an enantiornithine based on the presence of the following features: proximally forked and distally constricted pygostyle with ventrolateral processes; 'Y'-shaped, dorsolaterally excavated furcula; convex lateral margin of the coracoid; proximal humerus, rising dorsally and ventrally to centrally on the concave head; minor metacarpal projecting distally farther than the major metacarpal; and distal tarsals fused to the metatarsals, with metatarsals unfused along their lengths. The specimen differs from all other enantiornithines in the presence of enlarged teeth with grooves on the lingual surface (Fig. 8) and a unique combination of morphological features, therefore, we erect the new taxon *Sulcavis georum*, gen. et sp. nov.

Enantiornithine systematics are notoriously poorly resolved; however, we placed the new specimen into the latest available Mesozoic bird data set (O'Connor et al., 2011a) in order to test its placement as an enantiornithine and explore a possible relationship with the superficially similar *Shenqiornis mengi*. A total of 64 taxa were scored for 245 characters, with Dromaeosauridae as the outgroup; 31 characters were treated as ordered and all characters were weighted equally (see Supplemental Data). Any feature of BMNH Ph-000805 described as equivocal (i.e., postorbital) was scored as missing data. The analysis was run using TNT (Goloboff et al., 2008). We conducted a heuristic search retaining the single shortest tree from every 1000 trees followed by an additional round of tree bisection and reconnection (TBR) branch swapping. This analysis produced 144 shortest trees (length = 835 steps; consistency index = 0.389; retention Index = 0.670). The Nelson strict consensus tree (Fig. 9) resolves *Sulcavis* as an enantiornithine more derived than the longipterygids, in a polytomy with *Iberomesornis*, *Otogornis*, and two clades of derived enantiornithines including the 'avisaurids'; *Shenqiornis* forms the sister taxon to this clade. Bremer support for this hypothesis is low (Fig. 9), but this is unfortunately characteristic of Mesozoic bird cladistic analyses and is an issue beyond the scope of this paper (O'Connor and Zhou, 2012).

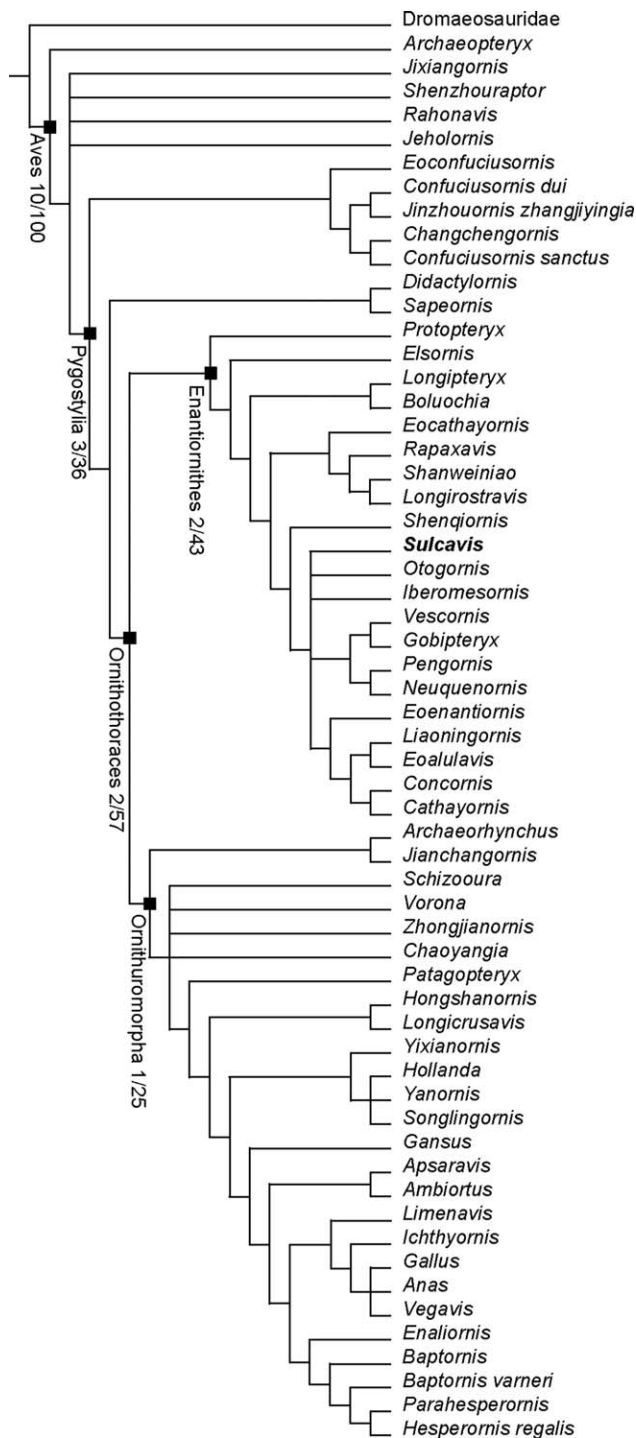


FIGURE 9. Cladogram of the strict consensus tree (length, 835 steps; consistency index = 0.389; retention index = 0.670) showing the hypothetical phylogenetic relationships of these Mesozoic birds. Note that *Shenqiornis* is resolved as sister taxon to a polytomy formed by *Sulcavis*, *Otogornis*, *Iberomesornis*, and two clades of derived enantiornithines. Absolute/relative Bremer supports are indicated at major nodes.

Trophic Inferences

No previously recognized avian specimen is known to possess any form of enamel ornamentation or specialization. BMNH Ph-000805 preserves longitudinal grooves on the lingual surface

of its premaxillary teeth (Fig. 8); similar features, although unknown among birds, are observed in numerous organisms, both close (e.g., theropod teeth referred to as “*Paronychodon*”) and distant relatives (e.g., globidensine mosasaurs) (Gilmore, 1912; Hwang, 2005). The presence of this feature in BMNH Ph-000805 is of uncertain significance—there are several possible explanations for the grooves that without additional specimens are difficult to differentiate (e.g., abnormal growth vs. true feature). If the grooves actually had a specific function, this would imply active selection and indicate that teeth played a unique role in this lineage of enantiornithines. This is unsurprising given the diversity of dental morphologies and the absence of edentulous enantiornithines in the Early Cretaceous (O’Connor and Chiappe, 2011). A number of sympatric basal ornithuromorph species are edentulous (e.g., *Schizooura lii*, *Hongshanornis longicresta*, *Archaeorhynchus spathula*), and the recognized diversity of dental morphologies among basal ornithuromorphs is low. Such a discrepancy in dental disparity suggests trophic differences between enantiornithines and ornithuromorphs, a suggestion further supported by the widespread presence of gastroliths among the latter (e.g., *Archaeorhynchus spathula*, *Yanornis martini* Zhou and Zhang, 2001, *Hongshanornis longicresta*) (Zhou et al., 2004; Zhou and Zhang, 2005, 2006b) and their complete absence in any known specimen of enantiornithine. Teeth are energetically costly structures and contribute weight to the skeleton—thus their large size and diversity in enantiornithines suggest active function. Mesozoic birds, however, show an overall trend towards tooth reduction, with the complete loss of teeth occurring independently at least four times (Louchart and Viriot, 2011). This may be linked to the development of the beak, which replaced the importance of teeth in the manipulation of food, and the presence of a well-developed gizzard (Louchart and Viriot, 2011). A gizzard is inferred to be present in at least two groups of Mesozoic birds (Sapeornithiformes, Ornithuromorpha), as well as in closely related groups of non-avian theropod dinosaurs (Oviraptorosauria, Ornithomimosauria), through the preservation of gastroliths (Zheng et al., 2011). The phylogenetic distribution of this feature and limited preservation in known taxa (i.e., *Sapeornis*) suggests that its absence in other groups may be taphonomic. However, both confuciusornithiforms and enantiornithines are known from hundreds of specimens from the same deposits, yet not one specimen preserves gastroliths. Recent studies also suggest that the appearance of a rhamphotheca on the rostrum may have inhibited tooth formation, and thus the evolution of the beak and the loss of teeth are interconnected (Louchart and Viriot, 2011). The sheer number of times this has occurred within Aves suggests a plesiomorphic weakness in avian odontogenetic pathways (Louchart and Viriot, 2011). These studies may suggest that enantiornithines did not possess a well-developed gizzard or that they were characterized by more stable odontogenesis. This highlights a major trophic difference between the two ornithothoracine clades: whereas ornithurines may have evolved to rely on a horny beak for food manipulation, enantiornithines retained teeth, and the diversity of dental shapes may reflect differences in food items between taxa.

The large, recurved, and laterally compressed teeth of *Longipteryx* are inferred to represent a carnivorous diet such as piscivory. *Pengornis houi* Zhou, Clarke, and Zhang, 2008, a large basal enantiornithine, possesses numerous small, blunt, low-crowned teeth that are interpreted for a diet of soft food items such as arthropods (O’Connor and Chiappe, 2011). The teeth of BMNH Ph-000805 are similar to those in *Shenqiornis mengi*, in which they have been interpreted as indicative of a durophagous diet, relative to other enantiornithines (O’Connor and Chiappe, 2011). Comparable enamel macrostructures have been reported in non-avian durophagous taxa such as the globidensine mosasaurs, whose bulbous, low-crowned teeth bear longitudinal wrinkles (Gilmore, 1912; Sanders, 2000). This

suggests that this new enantiornithine taxon, *Sulcavis georum*, may have been especially well adapted for a diet of hard food items relative to other Jehol birds.

ACKNOWLEDGMENTS

We thank M. Walsh (Dinosaur Institute, Natural History Museum of Los Angeles County) for preparing the specimen and D. Goodreau (Dinosaur Institute) for producing the cast deposited in the collection of the Natural History Museum of Los Angeles County. We are also grateful to S. Abramowicz (Dinosaur Institute) for producing the photographs and assisting with the creation of the figures. This study was supported by donations of D. and G. Gee to the Dinosaur Institute.

LITERATURE CITED

- Baumel, J. J., and L. M. Witmer. 1993. Osteologia; pp. 45–132 in J. J. Baumel, A. S. King, J. E. Breazile, H. E. Evans, and J. C. Van den Berge (eds.), *Handbook of Avian Anatomy: Nomina Anatomica Avium*, second edition. Nuttall Ornithological Club, Cambridge, U.K.
- Cau, A., and P. Arduini. 2008. *Enantiophoenix electrophyla* gen. et sp. nov. (Aves, Enantiornithes) from the Upper Cretaceous (Cenomanian) of Lebanon and its phylogenetic relationships. *Atti della Società Italiana di Scienze Naturali e del Museo Civico di Storia Naturale di Milano* 149:293–324.
- Chiappe, L. M. 1992. Enantiornithine (Aves) tarsometatarsi and the avian affinities of the Late Cretaceous Avisauridae. *Journal of Vertebrate Paleontology* 12:344–350.
- Chiappe, L. M. 1993. Enantiornithine (Aves) tarsometatarsi from the Cretaceous Lecho Formation of northwestern Argentina. *American Museum Novitates* 3083:1–27.
- Chiappe, L. M. 1995. The phylogenetic position of the Cretaceous birds of Argentina: Enantiornithes and *Patagopteryx deferrariisi*; pp. 55–63 in D. S. Peters (ed.), *Acta Palaeornithologica*. Forschungsinstitut Senckenberg, Frankfurt, Germany.
- Chiappe, L. M. 2002. Basal bird phylogeny: problems and solutions; pp. 448–472 in L. M. Chiappe and L. M. Witmer (eds.), *Mesozoic Birds: Above the Heads of Dinosaurs*. University of California Press, Berkeley, California.
- Chiappe, L. M. 2007. *Glorified Dinosaurs: The Origin and Early Evolution of Birds*. John Wiley & Sons, Hoboken, New Jersey, 263 pp.
- Chiappe, L. M., and J. O. Calvo. 1994. *Nequenornis volans*, a new Late Cretaceous bird (Enantiornithes: Avisauridae) from Patagonia, Argentina. *Journal of Vertebrate Paleontology* 14:230–246.
- Chiappe, L. M., and C. A. Walker. 2002. Skeletal morphology and systematics of the Cretaceous Euenantiornithes (Ornithothoraces: Enantiornithes); pp. 240–267 in L. M. Chiappe and L. M. Witmer (eds.), *Mesozoic Birds: Above the Heads of Dinosaurs*. University of California Press, Berkeley, California.
- Chiappe, L. M., S. Ji, Q. Ji, and M. A. Norell. 1999. Anatomy and systematics of the Confuciusornithidae (Theropoda: Aves) from the Late Mesozoic of northeastern China. *Bulletin of the American Museum of Natural History* 242:1–89.
- Chiappe, L. M., J. Marugán-Lobón, S. Ji, and Z. Zhou. 2008. Life history of a basal bird: morphometrics of the Early Cretaceous *Confuciusornis*. *Biology Letters* 4:719–723.
- Dalla Vecchia, F. M., and L. M. Chiappe. 2002. First avian skeleton from the Mesozoic of northern Gondwana. *Journal of Vertebrate Paleontology* 22:856–860.
- Gilmore, C. W. 1912. A new mosasauroid reptile from the Cretaceous of Alabama. *Proceedings of the United States National Museum* 41:479–484.
- Goloboff, P. A., J. S. Farris, and K. C. Nixon. 2008. TNT, a free program for phylogenetic analysis. *Cladistics* 24:774–786.
- Hou, L., L. M. Chiappe, F. Zhang, and C.-M. Chuong. 2004. New Early Cretaceous fossil from China documents a novel trophic specialization for Mesozoic birds. *Naturwissenschaften* 91:22–25.
- Hwang, S. H. 2005. Phylogenetic patterns of enamel microstructure in dinosaur teeth. *Journal of Morphology* 266:208–240.
- Linnaeus, C. 1758. *Systema Naturae per Regna Tria Naturae, Secundum Classes, Ordines, Genera, Species, cum Characteribus, Differentiis, Synonymis, Locis*. Volume 1: Regnum Animale. Editio decima, reformata. Laurentii Salvii, Stockholm, 824 pp.
- Louchart, A., and L. Viriot. 2011. From snout to beak: the loss of teeth in birds. *Trends in Ecology and Evolution* 26:663–673.
- Martin, L. D. 1995. The Enantiornithes: terrestrial birds of the Cretaceous. *Acta Palaeornithologica* 181:23–36.
- Morschhauser, E., D. J. Varricchio, C.-H. Gao, J.-Y. Liu, X.-R. Wang, X.-D. Cheng, and Q.-J. Meng. 2009. Anatomy of the Early Cretaceous bird *Rapaxavis pani*, a new species from Liaoning Province, China. *Journal of Vertebrate Paleontology* 29:545–554.
- O'Connor, J. K., and L. M. Chiappe. 2011. A revision of enantiornithine (Aves: Ornithothoraces) skull morphology. *Journal of Systematic Palaeontology* 9:135–157.
- O'Connor, J. K., and Z.-H. Zhou. 2012. A redescription of *Chaoyangia beishanensis* (Aves) and a comprehensive phylogeny of Mesozoic birds. *Journal of Systematic Palaeontology*. DOI: 10.1080/14772019.2012.690455.
- O'Connor, J. K., L. M. Chiappe, and A. Bell. 2011a. Pre-modern birds: avian divergences in the Mesozoic; pp. 39–114 in G. D. Dyke and G. Kaiser (eds.), *Living Dinosaurs: The Evolutionary History of Birds*. J. Wiley & Sons, Hoboken, New Jersey.
- O'Connor, J. K., L. M. Chiappe, C.-H. Gao, and B. Zhao. 2011b. Anatomy of the Early Cretaceous enantiornithine bird *Rapaxavis pani*. *Acta Palaeontologica Polonica* 56:463–475.
- O'Connor, J. K., X.-R. Wang, L. M. Chiappe, C.-H. Gao, Q.-J. Meng, X.-D. Cheng, and J.-Y. Liu. 2009. Phylogenetic support for a specialized clade of Cretaceous enantiornithine birds with information from a new species. *Journal of Vertebrate Paleontology* 29:188–204.
- Sanders, P. M. 2000. Prismless enamel in amniotes: terminology, function, and evolution; pp. 92–106 in M. F. Teaford, M. M. Smith, and M. W. J. Ferguson (eds.), *Development, Function and Evolution of Teeth*. Cambridge University Press, Cambridge, U.K.
- Sanz, J. L., L. M. Chiappe, B. P. Pérez-Moreno, A. D. Buscalioni, J. J. Moratalla, F. Ortega, and F. J. Poyato-Ariza. 1996. An Early Cretaceous bird from Spain and its implications for the evolution of avian flight. *Nature* 382:442–445.
- Sanz, J. L., L. M. Chiappe, B. Pérez-Moreno, J. J. Moratalla, F. Hernández-Carrasquilla, A. D. Buscalioni, F. Ortega, F. J. Poyato-Ariza, D. Rasskin-Gutman, and X. Martínez-Delclòs. 1997. A nestling bird from the Lower Cretaceous of Spain: implications for avian skull and neck evolution. *Science* 276:1543–1546.
- Walker, C. A. 1981. New subclass of birds from the Cretaceous of South America. *Nature* 292:51–53.
- Wang, X.-R., J. K. O'Connor, B. Zhao, L. M. Chiappe, C.-H. Gao, and X.-D. Cheng. 2010. A new species of Enantiornithes (Aves: Ornithothoraces) based on a well-preserved specimen from the Qiaotou Formation of Northern Hebei, China. *Acta Geologica Sinica* 84:247–256.
- Zhang, F., and Z. Zhou. 2000. A primitive enantiornithine bird and the origin of feathers. *Science* 290:1955–1960.
- Zhang, F., Z. Zhou, L. Hou, and G. Gu. 2000. Early diversification of birds: evidence from a new opposite bird. *Kexue Tongbao* 45:2650–2657.
- Zheng, X.-T., L. D. Martin, Z.-H. Zhou, D. A. Burnham, F.-C. Zhang, and D. Miao. 2011. Fossil evidence of avian crops from the Early Cretaceous of China. *Proceedings of the National Academy of Sciences of the United States of America* 108:15904–15907.
- Zhou, S., Z.-H. Zhou, and J. K. O'Connor. 2012. A new toothless ornithurine bird (*Schizooura lii* gen. et sp. nov.) from the Lower Cretaceous of China. *Vertebrata Palasiatica* 50:9–24.
- Zhou, Z., and F. Zhang. 2001. Two new ornithurine birds from the Early Cretaceous of western Liaoning, China. *Chinese Science Bulletin* 46:1258–1264.
- Zhou, Z., and F. Zhang. 2004. A precocial avian embryo from the Lower Cretaceous of China. *Science* 306:653.
- Zhou, Z., and F. Zhang. 2005. Discovery of an ornithurine bird and its implication for Early Cretaceous avian radiation. *Proceedings of the National Academy of Sciences of the United States of America* 102:18998–19002.
- Zhou, Z.-H., and F.-C. Zhang. 2006a. Mesozoic birds of China—a synoptic review. *Vertebrata Palasiatica* 44:74–98.

- Zhou, Z.-H., and F.-C. Zhang. 2006b. A beaked basal ornithurine bird (Aves, Ornithurae) from the Lower Cretaceous of China. *Zoologica Scripta* 35:363–373.
- Zhou, Z., J. Clarke, and F. Zhang. 2008. Insight into diversity, body size and morphological evolution from the largest Early Cretaceous enantiornithine bird. *Journal of Anatomy* 212:565–577.
- Zhou, Z.-H., F.-C. Zhang, and Z.-H. Li. 2010. A new Lower Cretaceous bird from China and tooth reduction in early avian evolution. *Proceedings of the Royal Society of London B* 277:219–227.
- Zhou, Z., J. Clarke, F. Zhang, and O. Wings. 2004. Gastroliths in *Yanornis*: an indication of the earliest radical diet-switching and gizzard plasticity in the lineage leading to living birds. *Naturwissenschaften* 91:571–574.

Submitted February 20, 2012; revisions received July 30, 2012; accepted July 30, 2012.

Handling editor: Trevor Worthy.